JOURNAL OF AGRICULTURAL AND FOOD CHEMISTRY
ARTICLE

J. Agric. Food Chem. 2010, 58, 9549–9555 9549
DOI:10.1021/jf101010w

Protein Substitution Affects Glass Transition Temperature and Thermal Stability

NARESH K. BUDHAVARAM, JONATHAN A. MILLER, YING SHEN, AND JUSTIN R. BARONE*

Biological Systems Engineering Department, Virginia Tech, Blacksburg, Virginia 24061

When proteins are removed from their native state they suffer from two deficiencies: (1) glassy behavior with glass transition temperatures (T_g) well above room temperature and (2) thermal instability. The glassy behavior originates in multiple hydrogen bonds between amino acids on adjacent protein molecules. Proteins, like most biopolymers, are thermally unstable. Substituting ovalbumin with linear and cyclic substituents using a facile nucleophilic addition reaction can affect T_g and thermal stability. More hydrophobic linear substituents lowered T_g by interrupting intermolecular interactions and increasing free volume. More hydrophilic and cyclic substituents increased thermal stability by increasing intermolecular interactions. In some cases, substituents instituted cross-linking between protein chains that enhanced thermal stability. Internal plasticization using covalent substitution and external plasticization using low molecular weight polar liquids show the same protein structural changes and a signature of plasticization is identified.

KEYWORDS: Thermal properties; nucleophilic addition reaction; protein

INTRODUCTION

Unique to proteins is the richness of interactions available between two molecules. Proteins typically rely on covalent, ionic, hydrogen bonding, and hydrophobic interactions to dictate secondary, tertiary, and quaternary structure. In the native state, these interactions are optimized, producing a highly functional material that performs well with a moderate amount of hydration. For example, a bird feather has a density of 0.9 g/cm^3, a modulus of 5−10 GPa, and can be strained to 50% (*1*−*6*). When removed from the native state, for instance because of solution or thermal processing, these interactions appear to maximize, producing a material that maintains a high modulus and strength but realizes a very high glass transition temperature (T_g), high density, and low strain to break that makes them glassy and brittle at room temperature (*7*, *8*). This suggests that there is an optimal amount of intermolecular interaction and free volume able to absorb ambient hydration to produce a material that is light, stiff, and tough and that loss of the interactions and free volume makes an inferior material. Theory suggests that it is indeed the optimal assembly and configuration of the biopolymers over molecular to macroscopic length scales that is responsible for these properties (*9*, *10*).

In the absence of reorganizing the original structure, the brittle behavior of isolated proteins is overcome by plasticizing them with low molecular weight polar compounds that can include water, glycerol, ethylene glycol and its polymers, propylene glycol and its polymers, sorbitol, diethylene glycol-monomethyl ether, diethanolamine, and acylated monoglycerides (*7*, *11*−*19*). Plasticization comes at a large cost to strength and stiffness (*7*). Plasticizers decrease intermolecular interactions and increase free volume, which results in a decreased T_g and increased flexibility. The resulting structure is usually amorphous, displaying no diffraction pattern in an X-ray experiment (*20*). Native protein structures do not require plasticization to the high levels necessary with isolated protein structures, although they do require a small amount of hydration for proper function. The largest problem with plasticizers may be migration, which occurs naturally but is hastened by increased temperature or exposure to water because of their hydrophilic nature. Therefore, it would be advantageous to increase the flexibility and lower the T_g of proteins without large costs to strength and stiffness and without having a diffusible component in the product.

Proteins, like most biopolymers, are thermally unstable because most chemical side groups on amino acids are easily oxidized. Proteins can also be semicrystalline, but melting temperatures would be concurrent with degradation temperatures so it would not be possible to thermally process them alone (*21*−*23*). Most commodity polymers made from petroleum not only have good physical properties but some measure of thermal stability. This allows them to be easily processed through conventional thermal methods like extrusion and be able to function in the solid state over a wide range of temperatures. If physical properties could be matched with a protein-based polymer, it would also be advantageous to have some thermal stability in polymers made from proteins. Therefore, improving the thermal stability and glass to rubber behavior of proteins could create new horizons in using proteins in engineering applications.

It is hypothesized that proteins removed from their native state can achieve improved thermal properties by covalently attaching groups to the protein thereby (1) increasing free volume and lowering intermolecular interactions from the maximum amount, a process sometimes referred to as "internal plasticization", and (2) stabilizing degradable chemical groups. To test the hypothesis,

*To whom correspondence should be addressed. E-mail: jbarone@vt.edu.

Published on Web 08/13/2010

ovalbumin (OA), a "model" protein, is chemically substituted. Ovalbumin is considered a "model" protein because it contains 385 amino acids, 185 of which are polar and six are cysteine, and all amino acids are represented in reasonable amounts. Ovalbumin has a molecular weight of 49670 g/mol (*24*). OA can be made soluble or insoluble through control of its intermolecular cystine bonding (*25*). Ovalbumin has been described as 41% α-helix, 34% β-sheet, 13% random coil, and 12% β-turn (*26*). Therefore, OA is equally polar and nonpolar, has an even distribution of secondary structure with all forms present, and contains all the amino acids offering many potential chemistries for modification.

The Michael addition is a nucleophilic addition reaction between electron-rich nucleophiles and electron-poor electrophiles (*27*). Specifically, the protein contains nucleophilic primary (−NH_2) and secondary (−NH) amines and thiols (−SH) that add to electron-poor carbon−carbon double bonds in substituted olefins (CH_2=CH-A) (*28*−*31*). The reaction proceeds at room temperature and near neutral pH in water, making it a very facile and green reaction. The Michael addition reaction is finding increased use in biomedical polymers for this reason (*32*−*34*). The high nucleophilicity of amines and thiols means that no catalyst is required although a slightly basic solution can increase kinetics (*31*). The easiest way to control the reaction is through pH because the first step of the Michael addition is to deprotonate the nucleophile (*27*). Each nucleophilic side group has a different dissociation constant, pK_R. Depending on the chemistry of A on the electrophile, the functionality of the protein can be altered. Depending on the size of A, the ability of two protein molecules to interact with one another could be affected as could the amount of free volume. Protein substitution using the Michael addition reaction has been reported previously but with different intents. Friedman modified bovine serum albumin (BSA) with methyl and ethyl vinyl sulfones to change the molecular weight so the substituted proteins would elute differently than pure proteins in a chromatography experiment (*28*, *29*). Ranucci et al. modified BSA and human serum albumin (HSA) by grafting poly(amido amine) chains onto the proteins without denaturing the protein for drug delivery applications (*30*). Sereikaite et al. modified BSA by cross-linking it with divinylsulfone (DVS) also for potential biomedical applications (*31*).

In this study, modification of ovalbumin protein through the Michael addition reaction has been investigated. OA has been covalently modified using ethyl vinyl sulfone (EVS) and acrylic acid (AA), both linear molecules, and butadiene sulfone (BS) and maleimide (MA), both cyclic molecules. The effect of substitution on OA thermal properties was investigated using differential scanning calorimetry (DSC) and thermogravimetric analysis (TGA). Structural changes were documented with Fourier transform-infrared (FT-IR) spectroscopy and X-ray powder diffraction (XRD).

EXPERIMENTAL PROCEDURES

Materials. Technical grade egg ovalbumin, dithiothreitol (DTT), reagent grade BS (mol wt 118.15 g/mol), AA (mol wt 72.01 g/mol), and MA (mol wt 97.07 g/mol) were purchased from Sigma Aldrich (USA). Dialysis membranes with 3500 g/mol molecular weight cut off and 95% EVS (mol wt 120.17 g/mol) were obtained from VWR (USA). All of the materials were used as obtained without any further modifications.

Substitution. First, 5 g of OA was added to 50 mL of deionized water. Then the pH was adjusted to 9 using borate buffer solution. To this solution, 0.0017 g (equivalent to moles of cysteine present on OA) DTT was added and the solution stirred for 30 min producing soluble OA (*35*). At this point, various concentrations of substituents were added to the OA solution and further stirred at 30 °C for 24 h. The substituent level was determined by the amount of deprotonated to protonated nucleophile on the amino acid side group, i.e., $[NH_2]/[NH_3^+]$ or $[S^-]/[SH]$. For OA, the lysine primary amines (K, pK_R = 10.8), cysteine thiols (C, pK_R = 8.3), and histidine secondary amines (H, pK_R = 6.0) yielded 12.6 potential reactive groups (PRG) per OA molecule at pH 9. The amines of asparagine (N) and glutamine (Q) were not counted because of the poor acid/base properties of the amide side groups although this may not be entirely true (*36*). The side group of arginine (R) was not counted because the side group dissociation constant, pK_R, was 12.5, yielding very little potential deprotonated groups for nucleophilic addition. Finally, the secondary amine of the α-carbon was assumed highly inaccessible because of its position on the protein main chain and potential to hydrogen bond to another main chain. The N-terminus of the OA molecule was omitted because of potential postsynthetic modification yielding unreactive groups.

Addition of EVS, BS, and MA did not affect pH. Addition of AA reduced the solution pH to 4 and 4N NaOH was added to adjust pH back to 9. The solutions were then dialyzed against deionized water for 24 h and the water was changed every 12 h. The dialyzed solution was poured onto Teflon-coated aluminum foil and dried at ambient conditions. During reaction, the EVS and BS solutions gelled. Water was added to the gelled solution and stirred for 1 h before dialysis. The dried samples were ground into fine powders using a mortar and pestle.

Nitrogen Analysis. To determine reaction yields of substituted OA, nitrogen analysis was performed using an Elementar Vario MAX CNS analyzer (Hanau, Germany). The reaction yield was determined by comparing the experimentally determined amount of nitrogen to the expected amount of nitrogen as the protein was substituted.

Thermal Analysis. Thermal analysis was performed on 8−10 mg samples in a nitrogen atmosphere. Given the difficulties associated with thermal analysis of biopolymers, at least three samples were analyzed using three different instruments so the glass transition (T_g) and thermal degradation (T_d) temperatures could be well-defined (*19*, *37*, *38*). The samples were analyzed on TA Instruments' SDT Q600 simultaneous DSC/TGA (differential scanning calorimeter/thermogravimetric analyzer), DSC Q100, and TGA Q500. For DSC, a two-cycle analysis was used. In the first cycle, the sample was equilibrated at 30 °C and then heated to 150 °C at a rate of 10 °C/min, equilibrated at 150 °C for 2 min, and then air-cooled to 30 °C. In the second cycle, the sample was heated to 300 °C at a rate of 10 °C/min. The glass transition temperatures were clearly defined, and good agreement was found between samples and instruments. For thermal stability analysis using TGA, the samples were heated to 600 °C at a rate of 10 °C/min.

Fourier Transform−Infrared (FT-IR) Spectroscopy. A Thermo-Nicolet 6700 FT-IR spectrometer with a Smart Orbit diamond ATR cell was used. The spectrum was collected with a total of 64 scans and a resolution of 4 cm^{-1} and then baseline corrected and smoothed. Deconvolution of the amide I band into individual components was accomplished with OMNIC v 7.3 software. The spectral region 1750−1590 cm^{-1} of the original spectrum was fitted with Gaussian/Lorentzian peaks. The number of peaks and their position were determined by the automatic peak finding feature of the program at low sensitivity and full width at half height of 3.857.

X-ray Powder Diffraction (XRD). XRD patterns were recorded on a PANalytical X'Pert PRO X-ray diffractometer (Westborough, MA) using Co radiation generated at 40 kV and 40 mA. Scanning was done with a Theta/Theta goniometer from 2 to 70° 2θ with a step size of 0.0668545° 2θ at a time of 600 s. The incident wavelength was λ = 0.179 nm.

RESULTS AND DISCUSSION

Glass Transition Temperature. The experimentally determined T_g of OA reduced with DTT was 221 °C, which was close to the value of 208 °C found by Katayama et al. for native OA using high ramp rate DSC (*38*). Discrepancies originated in our use of reduced OA, which would make more amino acids available for hydrogen bonding thus increasing T_g and a more typical, slower DSC heating rate for polymers. **Figure 1** shows the reduction of OA T_g with substitution. Lines are fits of the T_g data to the Couchman−Karasz equation, which has been shown to fit

biopolymer T_g data reasonably well

$$\ln\left(\frac{T_g}{T_{g,sg}}\right) = \frac{w_p \ln\left(\frac{T_{g,p}}{T_{g,sg}}\right)}{w_{sg}\left(\frac{T_{g,p}}{T_{g,sg}}\right) + w_p} \quad (1)$$

where w_p is the weight fraction of OA protein, w_{sg} is the weight fraction of substituted group (EVS, AA, BS, and MA), and $T_{g,p}$ is the glass transition temperature of OA, which was 494 K (221 °C) (*19*, *39*). The glass transition temperature of the substituted group, $T_{g,sg}$, was treated as a fitting parameter with $T_{g,sg}$ = 420, 465, 480, and 494 K providing the best fits for EVS, AA, BS, and MA data, respectively. For comparison, the plasticization of OA with glycerol is included, which is a fit of experimental data to eq 1(*19*). **Figure 1** shows that EVS covalently attached to OA was a very efficient plasticizer, even more so than glycerol, up to a mild degree of substitution. However, EVS could not reach the ultimate level of plasticization of glycerol, which was T_g reducing to room temperature. **Figure 1** has the ratio of substituent groups to potential reactive groups, [SG]/[PRG], plotted on the abscissa. Asymptotic behavior was observed after [SG]/[PRG] ~ 5−10, which could have indicated that the maximum amount of EVS had been added to OA and would not change T_g anymore. It also suggested that the original PRG calculation did not account for all reactive groups. The fitting parameter T_g = 420 K fit the data well in the [SG]/[PRG] ~ 0−10 range but not at higher ratios. AA and BS provided very little internal plasticization and MA none at all.

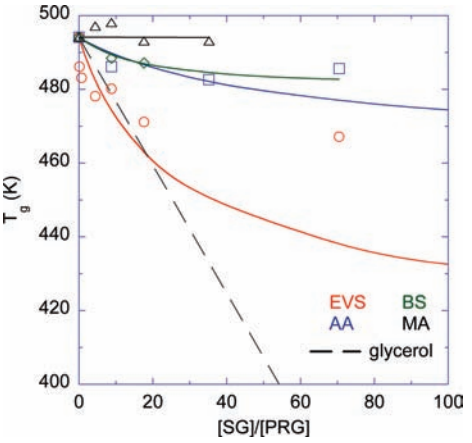

Figure 1. Change in glass transition temperature, T_g, with OA substitution. Symbols are experimental data and lines are fits to eq 1.

Thermal Stability. The first derivative of sample weight loss with temperature, dTGA, quantified the thermal stability of polymers by depicting two phenomena: the peak maximum was a measure of the overall degradation temperature, T_d, and the peak area was the rate of degradation. **Figure 2** shows the dTGA behavior for all of the substituted OA materials. The effect of substitution on T_d is shown in **Figure 3**. For EVS substituted OA, a new dTGA peak emerged around 285 °C with increasing EVS addition. The increase of the new dTGA peak was concurrent with the decrease of the primary dTGA peak around 320 °C, and the conservation of the two peaks meant no overall change in the degradation rate of OA-EVS. OA-BS showed peak broadening in this area (~285 °C). OA-EVS and

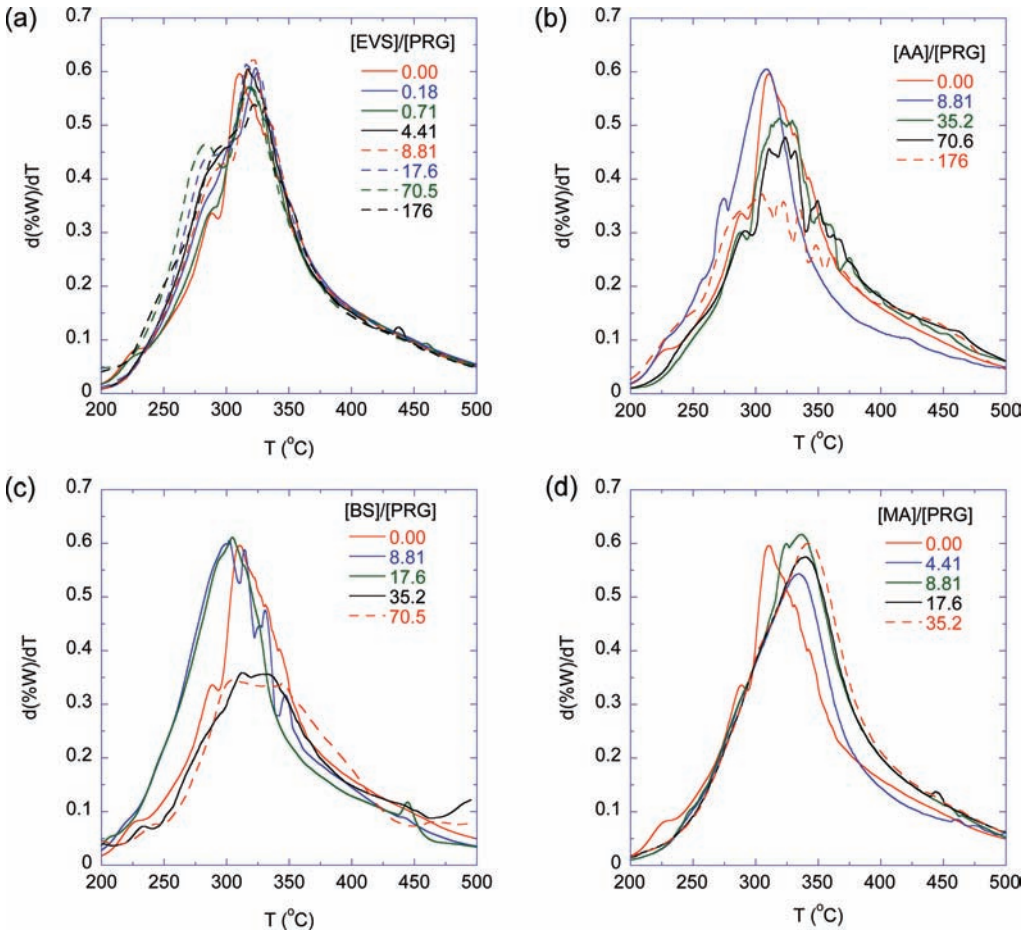

Figure 2. dTGA analysis of OA substituted with (**a**) EVS, (**b**) AA, (**c**) BS, and (**d**) MA.

OA-MA displayed a steady increase in T_d until saturating at [SG]/[PRG] ~ 6 with no significant change in degradation rate. OA-AA and OA-BS showed a decrease in T_d until [SG]/[PRG] ~ 8 then an increase in T_d until saturating at [SG]/[PRG] ~ 30, and it was upon the increase in T_d that the degradation rate decreased.

Structural Changes with Substitution. In the FT-IR spectra, the 1300−1200 cm^{-1} and 1150−1025 cm^{-1} regions were signature regions of the protein *and* substituent, making quantitative assessment of structure difficult (data not shown). The presence of substituent was easily discernible as sharper, more discrete peaks superimposed on top of broader protein peaks.

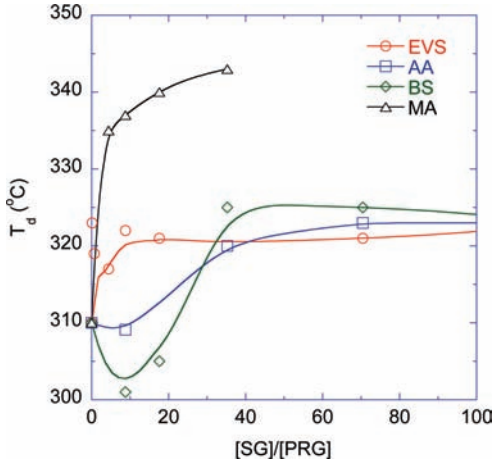

Figure 3. Change in thermal degradation temperature, T_d, with OA substitution.

Protein structural changes during plasticization manifested as changes in the amide I peak (*19*). Amide I described the state of protein carbonyls, mostly from the main chain, and were highly correlated with protein secondary structure (*40*). It was also sufficiently far from substituent peaks, with the AA carbonyl appearing at 1694 cm^{-1}, the MA carbonyl appearing at 1687 cm^{-1}, and ν(C═C) on EVS and BS appearing at 1611 cm^{-1}. As OA was substituted, the amide I or ν(C═O) peak around 1630 cm^{-1} broadened. The peak broadening originated in changing states of ν(C═O) on main chain amides, i.e., their participation in β-sheet, random coil, or α-helix conformations. The results of amide I peak deconvolution are shown in **Figure 4**. Included in each data set is the change in OA secondary structure between the native OA and reduced, solubilized, and solution cast OA. The native OA deconvolution results show the same β-sheet and random coil content as Ngarize et al. but less α-helix (*26*). In our deconvolution, we assigned peaks to β-turns at 1668 cm^{-1} and antiparallel β-sheets at 1683 cm^{-1}. As these structures and α-helix all appeared at the highest wavenumbers in the peak, our deconvolution added a contribution from antiparallel β-sheets while reducing the α-helix contribution. Predominantly, we were interested in the change in β-sheet relative to random coil, which described the maximum and minimum hydrogen bonding states, respectively, and therefore could potentially correlate with the glass transition. Upon reduction of OA, there was a loss of β-sheet structure with a concurrent and nearly equal increase in random coils. OA-AA and OA-MA had decreasing amounts of β-sheets with concurrent increasing amounts of random coils at [SG]/[PRG] ~ 0−10. There was then little change in the secondary structure at higher substitutions. At the highest degrees of substitution, i.e., [SG]/[PRG] > 30, all secondary structures saturated

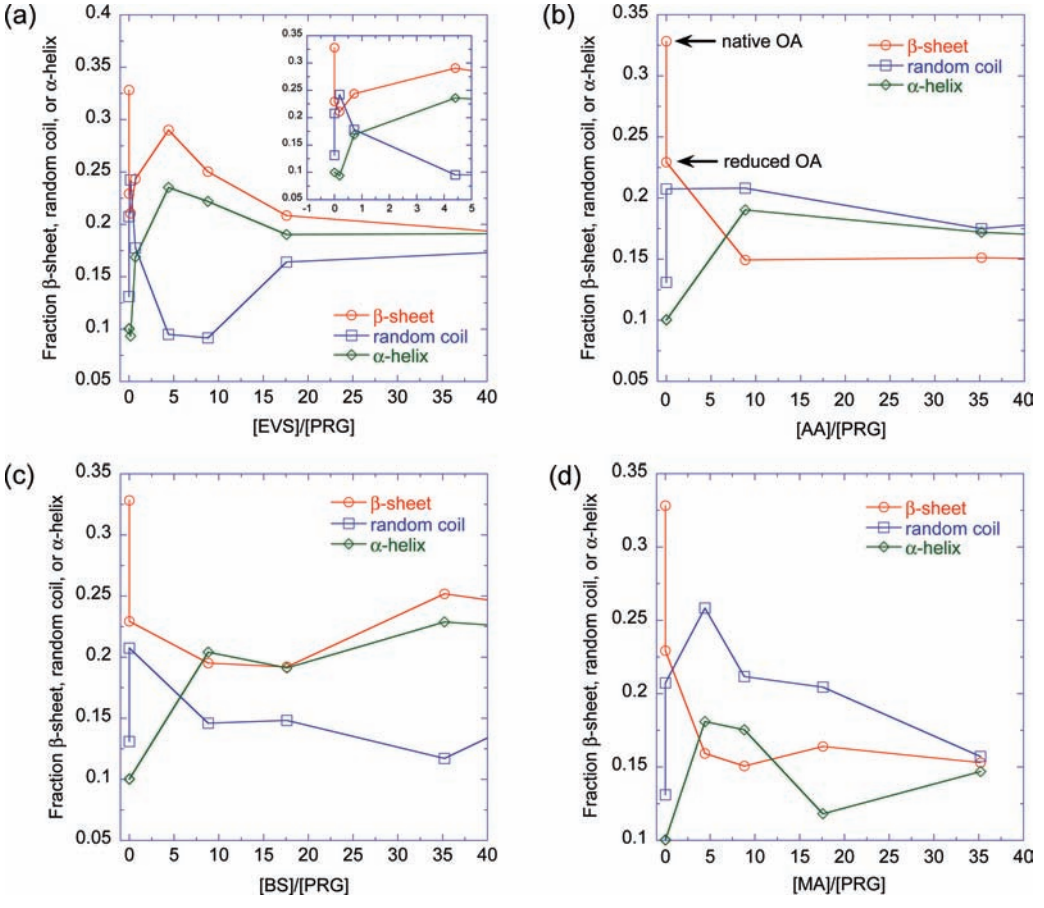

Figure 4. Results of amide I peak deconvolution for OA substituted with (**a**) EVS, (**b**) AA, (**c**) BS, and (**d**) MA.

at low values and FT-IR data showed that the materials were dominated by a high weight fraction of substituent. OA-BS displayed a decrease in β-sheets and random coils. OA-EVS exhibited the most complicated behavior with β-sheets decreasing slightly at the lowest substitution, increasing at moderate substitution, and then decreasing and finally saturating at higher substitutions with random coils doing the opposite.

The amide II peak around 1525 cm^{-1} described the state of primary and secondary amines on both the protein backbone and amino acid side groups (*41*). No substituent peaks appeared in this area, so changes were indicative of substitution on amines and protein structural changes. Amide II shifted lower in wavenumber for each substituted OA material as shown in **Figure 5**. Increasing substitution did not change OA-EVS or OA-MA, but OA-BS and OA-AA then shifted higher in wavenumber.

Diffraction patterns from OA and substituted OA materials were typical of semicrystalline proteins with two diffuse halos at Bragg spacings of about 0.46 and 1.10 nm (*42*). The 0.46 nm spacing represented the distance between two protein molecules in a native β-sheet independent of the protein's primary structure. The 1.10 nm spacing represented the intersheet distance between two stacked β-sheets and was a function of the shape and size of the amino acid side chains (*42*). The peaks were diffuse because of the nonuniform size of the β-sheets, their random arrangement in the powder diffraction experiment, and the presence of amorphous regions. The diffraction patterns for OA materials were normalized at the $2\theta = 9.5°$ or $d = 1.10$ nm peak for comparison. OA-EVS and OA-BS showed similar behavior. As substitution increased, the 1.10 nm peak broadened and the 0.46 nm peak sharpened and grew in intensity as exemplified by OA-EVS XRD patterns in **Figure 6a**. OA-AA did not show much change as shown in **Figure 6b**. The sharp peaks occurring at high substitution were consistent with crystallized acrylic acid (*43*).

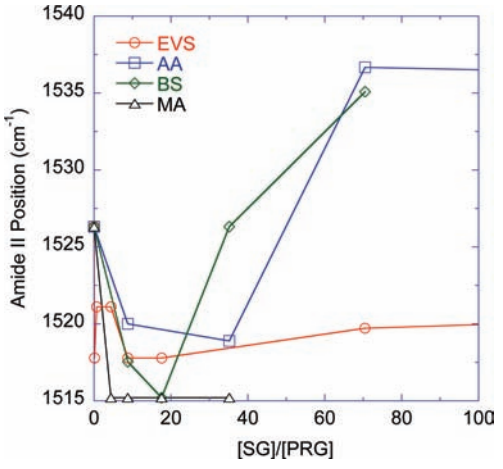

Figure 5. Change in amide II peak with OA substitution.

Structural Signatures of Plasticization and Thermal Stability. The observed thermal behavior can be directly correlated to the structural changes of the OA protein as various functionality was added. **Figure 7** shows the structure of each substituent added onto the protein. EVS added medium chain branching with a hydrophobic end, AA added short chain branching with a hydrophilic end, BS added a slightly hydrophilic ring, and MA added a more hydrophilic ring. By adding each onto OA, the native protein secondary, tertiary, and quarternary structures were modified.

The FT-IR and XRD results correlate with each other and are consistent with the idea of an overall loss of order and gain of disorder (*44*). It has been observed previously that the decrease in β-sheets and increase in random coils, as measured by amide I peak deconvolution, and the broadening of the 1.10 nm peak and sharpening of the 0.46 nm peak, as measured by XRD, correlate with increasing external plasticization of proteins by glycerol (*19*). OA-EVS exhibited both behaviors and had the largest T_g decrease so these trends may be a signature of the protein structural rearrangements necessary to transition from a glassy to a rubbery state. Taking the FT-IR and XRD data together, a potential mechanism could be that substitution first occurred at available side groups on random coils at [EVS]/[PRG] $\sim$ 0−5. The added free volume, manifesting as a decrease in T_g, allowed some of the previous random coils to now form β-sheets. In other words, there was more probability of two main chains finding each other to hydrogen bond. In the direction normal to the main chain on the side groups, any introduced β-sheets were now pushed apart, minimizing interactions in this direction. So free volume at low substitution was in the side group direction. Although there was an increase in β-sheets, the amount per unit volume was smaller than in the native state resulting in the T_g decrease. Further substitution, i.e., [EVS]/[PRG] $\sim$ 5−20 occurred on side groups *and* on main chain amines, both of which were available for reaction in solution. There was then a decrease in β-sheets and an increase in random coils, with free volume introduced between main chains and in the side group direction and a further decrease in T_g. At these substitution levels, the chains had very little interaction with each other, so the interactions per unit volume were small resulting in a low T_g. At [EVS]/[PRG] > 20, no further decrease in T_g occurred. This was also the region where no further changes in the FT-IR amide I and II were observed. The limited internal plasticization of OA with

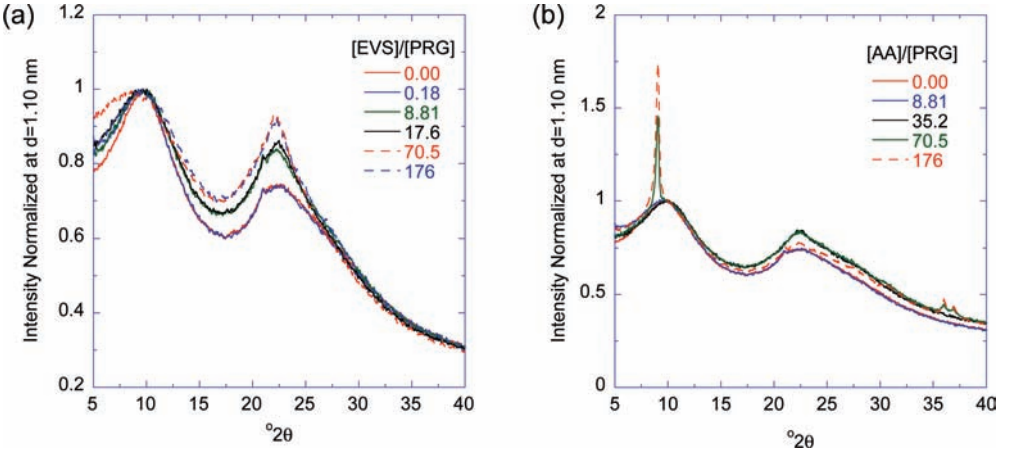

Figure 6. XRD results for OA substituted with (**a**) EVS and (**b**) AA.

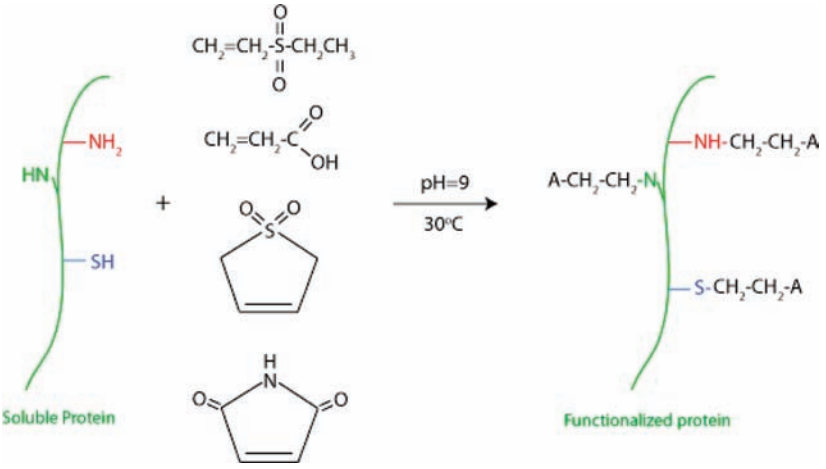

Figure 7. Chemical structure of substituents and schematic depicting how electron poor vinyl groups add to electron rich amines and thiols on the protein.

EVS appeared related to the ability to continue to substitute. Elemental analysis showed that the yield decreased to 70% at [SG]/[PRG] ~ 25 and then dropped precipitously. Further changes in the XRD could be related to excess EVS aggregating around the protein, which were not manifesting as protein changes at all. Sharp peaks in the OA-AA and OA-BS XRD patterns at high substitution support the theory that excess substituent aggregated or crystallized around the protein and was too large or too bound to diffuse during dialysis.

OA-AA and OA-BS exhibited less pronounced changes in protein secondary structure, and the limited reduction of T_g appeared to be related to this. In addition, AA added more hydrogen bonding potential to the protein and any structural change could be compensated for by more hydrogen bonding. BS added stiffness to the protein chain that again could compensate for any structural changes to maintain T_g. The addition of MA disrupted β-sheets and increased random coil content. Again, the chain stiffness added by the ring compensated for this resulting in no T_g change.

Unlike the EVS system, the potential for interactions between protein molecules substituted with AA, BS, or MA was high. For AA, it was through hydrogen bonding interactions forming AA dimers (*43*, *45*). For BS and MA, it was through cross-linking across the C=C bond in the ring (*46*−*50*). These interactions, along with the ring structure of BS and MA, maintained the high glass transition temperature of the protein even though the native protein structure was disrupted. These interactions also had an influence on the thermal stability of the protein. Triethanolamine plasticized soy protein displayed an increased thermal stability because of the increased hydrogen bonding interactions between the components (*51*). Maleimide and sulfone have been used to stabilize thermoplastic polymers to high temperature (*52*, *53*). In this study, the sulfones did not impart thermal stability, instead causing degradation at ~285 °C, which was lower than the native protein but higher than some thermoplastic materials. Thermal stability was imparted through increased protein−protein interactions. The smaller changes in amide I in FT-IR analysis for these materials showed that more intermolecular interactions were contributing to thermal stability. The fact that MA did not have marked decreases in thermal degradation rate could be because it had 2 C=O and 1 N−H on the ring that maintained degradation rate regardless of the shift in T_d with intermolecular interactions. However, there was spectroscopic evidence that OA-MA intermolecular interactions may not have been as strong as OA-AA and OA-BS intermolecular interactions. OA-AA and OA-BS displayed shifting in amide II at the same points in substitution that reduced thermal degradation was observed, indicating that this may be a signature of the strongest intermolecular interactions. Amide I described protein conformational changes, which influenced glass transition temperature. Amide II appeared more dependent on chemical substitution. Because amide II originated in primary and secondary amines, it was more representative of the actual substitution rather than protein conformational changes. All samples shifted to lower wavenumber with substitution before saturating at [SG]/[PRG] ~ 10. The shifting to lower wavenumber was consistent with the disappearance of primary amines, which was the dominant reactive site on the protein (*41*). The correlation between the changes in thermal degradation temperature and amide II position suggested that substitution alone was the larger influence on thermal stability and that it could be described by the amide II behavior.

It was shown that a simple nucleophilic addition reaction could be used to substitute proteins in aqueous solution at room temperature to affect protein thermal properties. Glass transition temperature could be reduced through linear substituents with hydrophobic ends and thermal stability increased by increasing hydrogen bonding or covalent interactions between proteins. FT-IR spectroscopy and XRD quantitatively described changes in the structure of the proteins that correlated with changes in the glass transition temperature and thermal stability. Although it was possible to reduce the glass transition, external plasticization was still more practical to reduce T_g to a point where a flexible material at room temperature would be expected.

LITERATURE CITED

(1) Purslow, P. P.; Vincent, J. F. V. Mechanical properties of primary feathers from the pigeon. *J. Exp. Biol.* **1978**, *72*, 251–260.
(2) Fraser, R. D. B.; MacRae, T. P. Molecular structure and mechanical properties of keratins. In *Symposia of the Society for Experimental Biology, No. XXXIV, The Mechanical Properties of Biological Materials*; Vincent, J. F. V., Currey, J. D., Eds.; Cambridge University Press: New York, 1980; pp 211−246.
(3) Bonser, R. H. C. The mechanical properties of feather keratin. *J. Zool.* (*London*) **1996**, *239*, 477–484.
(4) Bonser, R. H. C.; Farrent, J. W. Influence of hydration on the mechanical performance of duck down feathers. *Br. Poult. Sci.* **2001**, *42*, 271–273.
(5) Bonser, R. H. C.; Purslow, P. P. The Young's modulus of feather keratin. *J. Exp. Biol.* **1995**, *198*, 1029–1033.
(6) Taylor, A. M.; Bonser, R. H. C.; Farrent, J. W. The influence of hydration on the tensile and compressive properties of avian keratinous tissues. *J. Mater. Sci.* **2004**, *39*, 939–942.
(7) Barone, J. R.; Schmidt, W. F.; Liebner, C. F. E. Thermally processed keratin films. *J. Appl. Polym. Sci.* **2005**, *97*, 1644–1651.

(8) Fischer, H.; Polikarpov, I.; Craievich, A. F. Average protein density is a molecular weight dependent function. *Protein Sci.* **2004**, *13*, 2825–2828.
(9) de Gennes, P.-G.; Okumura, K. On the toughness of biocomposites. *C. R. Acad. Sci., Ser. IV: Phys.−Astrophys.* **2000**, *1*, 257–261.
(10) Okumura, K. Fracture strength of biomimetic composites: scaling views on nacre. *J. Phys.: Condens. Matter* **2005**, *17*, S2879–S2884.
(11) Gennadios, A.; Weller, C. L.; Testin, R. F. Property modification of edible wheat gluten-based films. *Trans. ASAE* **1993**, *36*, 465–470.
(12) Sanchez, A. C.; Popineau, Y.; Mangavel, C.; Larre, C.; Gueguen, J. Effect of different plasticizers on the mechanical and surface properties of wheat gliadin films. *J. Agric. Food Chem.* **1998**, *46*, 4539–4544.
(13) Pouplin, M.; Redl, A.; Gontard, N. Glass transition of wheat gluten plasticized with water, glycerol, or sorbitol. *J. Agric. Food Chem.* **1999**, *47*, 538–543.
(14) Cuq, B.; Boutrot, F.; Redl, A.; Lullien-Pellerin, V. Study of the temperature effect on the formation of wheat gluten network: influence on mechanical properties and protein solubility. *J. Agric. Food Chem.* **2000**, *48*, 2954–2959.
(15) Irissin-Mangata, J.; Bauduin, G.; Boutevin, B.; Gontard, N. New plasticizers for wheat gluten films. *Eur. Polym. J.* **2001**, *37*, 1533–1541.
(16) Krochta, J. M. Proteins as raw materials for films and coatings: definitions, current status, and opportunities. In *Protein-Based Films and Coatings*; Gennadios, A., Ed.; CRC Press LLC: Boca Raton, FL, 2002; pp 1−41.
(17) Kim, K. M.; Marx, D. B.; Weller, C. L.; Hanna, M. A. Influence of sorghum wax, glycerin, and sorbitol on physical properties of soy protein isolate films. *J. Am. Oil Chem. Soc.* **2003**, *80*, 71–76.
(18) Sothornvit, R.; Olsen, C. W.; McHugh, T. H.; Krochta, J. M. Formation conditions, water-vapor permeability, and solubility of compression-molded whey protein films. *J. Food Sci.* **2003**, *68*, 1985–1989.
(19) Athamneh, A.; Griffin, M.; Whaley, M.; Barone, J. R. Conformational changes and molecular mobility in plasticized proteins. *Biomacromolecules* **2008**, *9*, 3181–3187.
(20) Chen, P.; Zhang, L. New Evidences of Glass Transitions and Microstructures of Soy Protein Plasticized with Glycerol. *Macromol. Biosci.* **2005**, *5*, 237–245.
(21) Magoshi, J.; Magoshi, Y.; Nakamura, S.; Kasai, N.; Kakudo, M. Physical properties and structure of silk. V. Thermal behavior of silk fibroin in the random-coil conformation. *J. Polym. Sci., Polym. Phys. Ed.* **1977**, *15*, 1675–1683.
(22) Motta, A.; Fambri, L.; Migliaresi, C. Regenerated silk fibroin films: thermal and dynamic mechanical analysis. *Macromol. Chem. Phys.* **2002**, *203*, 1658–1665.
(23) Hu, X.; Kaplan, D.; Cebe, P. Determining beta-sheet crystallinity in fibrous proteins by thermal analysis and infrared spectroscopy. *Macromolecules* **2006**, *39*, 6161–6170.
(24) Nisbet, A. D.; Saundry, R. H.; Moir, A. J. G.; Fothergill, L. A.; Fothergill, J. E. The complete amino-acid sequence of hen ovalbumin. *Eur. J. Biochem.* **1981**, *115*, 335–345.
(25) Whitaker, J. R.; Tannenbaum, S. R. *Food Proteins*; AVI Publishing Company: Westport, CT, 1977.
(26) Ngarize, S.; Herman, H.; Adams, A.; Howell, N. Comparison of changes in the secondary structure of unheated, heated, and high-pressure-treated β-lactoglobulin and ovalbumin proteins using Fourier transform Raman spectroscopy and self-deconvolution. *J. Agric. Food Chem.* **2004**, *52*, 6470–6477.
(27) Mather, B. D.; Viswanathan, K.; Miller, K. M.; Long, T. E. Michael addition reactions in macromolecular design for emerging technologies. *Prog. Polym. Sci.* **2006**, *31*, 487–531.
(28) Friedman, M.; Finley, J. W. Reactions of proteins with ethyl vinyl sulfone. *Int. J. Pept. Protein Res.* **1975**, *7*, 481–486.
(29) Sid Masri, M.; Friedman, M. Protein reactions with methyl and ethyl vinyl sulfones. *J. Protein Chem.* **1988**, *7*, 49–54.
(30) Ranucci, E.; Bignotti, F.; Luca Paderno, P.; Ferruti, P. Modification of albumins by grafting poly(amido amine) chains. *Polymer* **1995**, *36*, 2989–2994.
(31) Sereikaite, J.; Bassus, D.; Bobnis, R.; Dienys, G.; Bumeliene, Z.; Bumelis, V.-A. Divinyl sulfone as a crosslinking reagent for oligomeric proteins. *R. J. Bioorg. Chem.* **2003**, *29*, 227–230.
(32) Elbert, D. L.; Hubbell, J. A. Conjugate addition reactions combined with free-radical cross-linking for the design of materials for tissue engineering. *Biomacromolecules* **2001**, *2*, 430–441.
(33) Bergman, K.; Hilborn, J.; Bowden, T. Selective Michael-type addition of D-glucuronic acid derivative in the synthesis of model substances for uronic acid containing polysaccharides. *eXPRESS Polym. Lett.* **2008**, *2*, 553–559.
(34) Peng, X. C.; Peng, X. H.; Liu, S. M.; Zhao, J. Q. Synthesis and properties of new amphoteric poly(amidoamine) dendrimers. *eXPRESS Polym. Lett.* **2009**, *3*, 510–517.
(35) Dicharry, R. M.; Ye, P.; Saha, G.; Waxman, E.; Asandei, A. D.; Parnas, R. S. Wheat gluten-thiolated poly(vinyl alcohol) blends with improved mechanical properties. *Biomacromolecules* **2006**, *7*, 2837–2844.
(36) Friedman, M. Applications of the ninhydrin reaction for analysis of amino acids, peptides, and proteins to agricultural and biomedical sciences. *J. Agric. Food Chem.* **2004**, *52*, 385–406.
(37) Micard, V.; Guilbert, S. Thermal behavior of native and hydrophobized wheat gluten, gliadin and glutenin-rich fractions by modulated DSC. *Int. J. Biol. Macromol.* **2000**, *27*, 229–236.
(38) Katayama, D. S.; Carpenter, J. F.; Manning, M. C.; Randolph, T. W.; Setlow, P.; Menard, K. P. Characterization of amorphous solids with weak glass transitions using high ramp rate differential scanning calorimetry. *J. Pharm. Sci.* **2008**, *97*, 1013–1024.
(39) Barone, J. R.; Medynets, M. Thermally processed levan polymers. *Carbohydr. Polym.* **2007**, *69*, 554–561.
(40) Jackson., M.; Mantsch, H., H. Protein secondary structure from FT-IR spectroscopy: correlation with dihedral angles from three-dimensional Ramachandran plots. *Can. J. Chem.* **1991**, *69*, 1639–1642.
(41) Gunzler, H.; Gremlich, H.-U. *IR Spectroscopy: An Introduction*; WILEY-VCH: Weinheim, Germany, 2002.
(42) Fraser, R. D. B.; MacRae, T. P. *Conformation in Fibrous Proteins and Related Synthetic Polypeptides*; Academic Press: New York, 1973.
(43) Higgs, M. A.; Sass, R. L. The crystal structure of acrylic acid. *Acta Crystallogr.* **1963**, *16*, 657–661.
(44) Kreplak, L.; Doucet, J.; Dumas, P.; Briki, F. New Aspects of the α-Helix to β-Sheet Transition in Stretched Hard α-Keratin Fibers. *Biophys. J.* **2004**, *87*, 640–647.
(45) Aminova, R. M.; Schamov, G. A.; Aganov, A. V. Calculation of the structure and nuclear magnetic shielding constants of some H-bonded carbon acid complexes. *J. Mol. Struct. (THEOCHEM)* **2000**, *498*, 233–246.
(46) Durmaz, H.; Dag, A.; Gursoy, D.; Demirel, A. L.; Hizal, G.; Tunca, U. Multiarm star triblock terpolymers via sequential double click reactions. *J. Polym. Sci., Part A: Polym. Chem.* **2010**, *48*, 1557–1564.
(47) Goethals, E. J. On the polymerization and copolymerization of sulfolenes. *Makromol. Chem.* **1967**, *109*, 132–142.
(48) Hacioglu, B.; Suzer, S.; Akbulut, U.; Toppare, L.; Aybar, P.; Utley, J. H. P. Characterization of electroinitiated and radiation polymerized poly(butadiene sulfone). *J. Macromol. Sci., Part A: Pure Appl. Chem.* **1991**, *A28*, 329–345.
(49) Aybar, P.; Hacioglu, B.; Akbulut, U. Electroinitiated polymerization of butadiene sulfone. *J. Polym. Sci., Part A: Polym. Chem.* **1991**, *29*, 1971–1976.
(50) Smith, M. E. B.; Schumacher, F. F.; Ryan, C. P.; Tedaldi, L. M.; Papioannou, D.; Waksman, G.; Caddick, S.; Baker, J. R. Protein modification, bioconjugation, and disulfide bridging using bromomaleimides. *J. Am. Chem. Soc.* **2010**, *132*, 1960–1965.
(51) Tian, H.; Liu, D.; Zhang, L. Structure and properties of soy protein films plasticized with hydroxyamine. *J. Appl. Polym. Sci.* **2009**, *111*, 1549–1556.
(52) Yukawa, S.; Omayu, A.; Matsumoto, A. Thermally stable fluorescent maleimide/isobutene alternating copolymers containing pyrenyl and alkynpyrenyl moieties in the side chain. *Macromol. Chem. Phys.* **2009**, *210*, 1776–1784.
(53) Fahmy, M. M. Inhibition of the thermal degradation of rigid poly(vinyl chloride) using poly(*N*-[4-(*N*′-phenyl amino carbonyl)phenyl]maleimide). *J. Appl. Polym. Sci.* **2010**, *115*, 2013–2018.

Received for review March 16, 2010. Revised manuscript received July 7, 2010. Accepted July 28, 2010. This work was supported by the U.S. Poultry and Egg Association and the USDA/CSREES funded Virginia Tech Biodesign and Bioprocessing Research Center.